THE JOURNAL OF BIOLOGICAL CHEMISTRY VOL. 286, NO. 51, pp. 43881–43890, December 23, 2011

Conformational Dynamics of the Plug Domain of the SecYEG Protein-conducting Channel

Received for publication, August 24, 2011, and in revised form, October 20, 2011 Published, JBC Papers in Press, October 27, 2011, DOI 10.1074/jbc.M111.297507

Jelger A. Lycklama a Nijeholt, Zht Cheng Wu, and Arnold J. M. Driessen[1]

From the Molecular Microbiology, Groningen Biomolecular Sciences and Biotechnology institute, and the Zernike Institute for Advanced Materials, University of Groningen, 9747 AG Groningen, The Netherlands

Background: The translocon mediates the translocation and insertion of proteins across and into the membrane.
Results: The plug domain that seals the channel clears a vectorial path during protein translocation but remains at its initial position during the insertion of hydrophobic transmembrane segments.
Conclusion: The translocon undergoes different conformational changes depending on its mode of functioning.
Significance: Insight is made into the conformational dynamics of the translocon.

The central pore of the SecYEG preprotein-conducting channel is closed at the periplasmic face of the membrane by a plug domain. To study its conformational dynamics, the plug was labeled site-specifically with an environment-sensitive fluorophore. In the presence of a stable preprotein translocation intermediate, the SecY plug showed an enhanced solvent exposure consistent with a displacement from the hydrophobic central pore region. In contrast, binding and insertion of a ribosome-bound nascent membrane protein did not alter the plug conformation. These data indicate different plug dynamics depending on the ligand bound state of the SecYEG channel.

In *Escherichia coli* and other bacteria, many proteins need to pass or insert into the cytoplasmic membrane to reach their functional location. This process involves the translocon, a complex of three membrane proteins (the SecYEG complex) that together form a protein-conducting channel in the membrane (1). Most secretory proteins (preproteins) are translocated across the cytoplasmic membrane by the translocon in a post-translational manner. This process involves the SecA motor protein that employs multiple cycles of ATP binding and hydrolysis to thread the unfolded polypeptide chain in a stepwise fashion through the SecYEG channel. Membrane proteins are mostly inserted co-translationally into the membrane by the translocon. Herein, the emerging ribosome nascent membrane protein (RNC)[2] is recognized by the signal recognition particle and targeted to its membrane receptor FtsY that is bound to the SecYEG complex. The signal recognition particle and FtsY heterodimerize, causing the activation of their GTPase activity that in turn induces the release of the RNC to the translocon. At that stage, translation continues, and the insertion of the newly synthesized membrane protein via the translocon is completed.

In recent years, the structure of the translocon from different microbial sources has been elucidated yielding major new insights in its possible functioning. In the crystal structure of the *Methanocaldococcus jannaschii* SecYEβ, the main channel subunit SecY consists of 10 α-helical transmembrane segments (TMS). TMS1–5 and TMS6–10 are pseudosymmetrically opposed to each other, resembling a clamshell (2). The channel is constricted in the middle, where six hydrophobic residues are aligned to form a ring, which is proposed to form a tight seal around the translocating polypeptide that prevents the leakage of ions (3). The structure suggests the presence of a membrane entry pathway via a lateral gate that is formed by at least TMS2b and -7. When the channel is opened, the lateral gate will expose the central aqueous pore to the lipid bilayer thereby providing a possible exit path for hydrophobic transmembrane segments. SecE envelops the SecY channel in a V-shaped manner, providing stability to the complex. The third subunit SecG or Secβ is located peripherally to the heterotrimeric translocation channel.

In a cross-section, the protein-conducting channel has an hourglass shape, but it is blocked at the periplasmic face of the membrane by a small helical segment. This region is termed the plug and resides closely to the hydrophobic constriction ring in the *M. jannaschii* SecYEβ structure, which likely represents the "closed" state of the channel. Movement of the plug domain is necessary to clear a vectorial translocation path for preproteins across the membrane. Although previous *in vivo* and *in vitro* cross-linking studies proposed that the plug domain could move entirely to the outside of the channel upon protein translocation (4, 5), only a relatively small movement of the plug domain is sufficient to allow for translocation (6).

In the yeast Sec61p complex that is homologous to the SecYEG complex, deletion of the plug domain had little influence on cell viability; however, the efficiency of protein translocation decreased (7). In the *E. coli* SecYEG complex, deletion of the plug domain renders the complex thermolabile, but translocation is not inhibited (8). The lack of a strong phenotype has been attributed to a compensatory effect of other loops taking a similar position of the original plug (9). Plug deletion mutants allow the translocation of preproteins with a defective or missing signal sequences in an analogous manner as the PrlA

[1] To whom correspondence should be addressed: Nijenborgh 7, 9747 AG, Groningen, The Netherlands. Tel.: 31-50-3632164; Fax: 31-50-3632154; E-mail: a.j.m.driessen@rug.nl.

[2] The abbreviations used are: RNC, ribosome nascent membrane protein; TMS, transmembrane segments; IMV, inner membrane vesicles; NBD, *N*-((2-(Iodoacetoxy)ethyl)-*N*-methyl)amino-7-nitrobenz-2-oxa-1,3-diazole; DDM, β-D-dodecylmaltoside; AMP-PNP, adenosine 5′-(β,γ-imino)triphosphate; DHFR, dihydrofolate reductase; NaTT, sodium tetrathionate.

suppressor mutations in and around the constriction ring (10). Such suppressor mutants exhibit an improved initiation of preprotein translocation (11), indicating that the plug domain is particularly important for the early stages of preprotein translocation. Molecular dynamics simulation studies suggest that the position of the plug domain depends on the polarity of the incoming polypeptide and thus for sorting of inserting preproteins and membrane proteins (12).

The structure of the *Thermotoga maritima* SecYEG with the bound SecA in an ATP hydrolysis transition state suggests that during the initial stages of channel opening, a widening of the lateral gate occurs that may provide space for the inserting signal sequence (13). In this state the plug domain already partially clears the translocation path and localizes to the periplasmic side of the lateral gate. This conformation is termed "pre-open state" as the lateral gate needs to open further to allow for preprotein translocation and activation of the SecA ATPase activity (14). In the SecYEβ structure of *Pyrococcus furiosus*, the C-terminal α-helical segment of a neighboring SecY molecule intrudes the channel of another SecY molecule. Remarkably, the structure shows an opening of the lateral gate, whereas the plug domain remains at its position facing the hydrophobic constriction ring, thus maintaining a tight membrane seal. This structure supports the idea that membrane segments can be inserted before the plug has vacated its central position (15). The crystal structure of the *Thermus thermophilus* SecYE with a bound anti-SecY Fab fragment shows only a partial opening of the lateral gate at the cytoplasmic side, also termed the hydrophobic crack (16). Also here, the plug domain remains at its central position. Recently, a cryo-EM structure was resolved showing the ribosome with a stalled nascent chain from the membrane protein FtsQ when bound to SecYEG in membrane-embedded nanodiscs (17). The structure revealed conformational changes in the cytoplasmic loops of SecY that interact with the ribosome and additionally suggested that the N-terminal signal anchor TMS from FtsQ is intercalated in the lateral gate. Compared with the pre-open state of the SecA bound SecYEG structure, the lateral gate has opened further to allow the occupation by the TMS. The plug domain, however, was not resolved in this lower resolution structure.

Although the structural studies provide snapshots of possible stages in the channel opening mechanism, little is known about the conformational dynamics of the SecYEG channel. Although the plug domain is not strongly hydrophobic, it resides in a relatively apolar environment when it occupies the central pore region. Movement of the plug away from the constriction should result in an increased exposure to water. Here we have used the environment-sensitive fluorophore to probe the polarity of a set of plug domain positions at different stages of the translocation reaction as a measure of its conformational state. Remarkably, the plug domain conformational dynamics seem to differ for SecA-mediated protein translocation and membrane insertion of ribosome-bound nascent membrane proteins. This suggests different roles of the plug domain during these two distinct modes of function of the translocon.

TABLE 1
Strains and plasmids used in this study

Strains/Plasmids	Characteristics	Source
E. coli DH5α	*supE44*, Δ*lacU169* (Δ*80lacZ_M15*) *hsdR17, recA1, endA1, gyrA96 thi-1, relA1*	(41)
E. coli SF100	F $^-$, Δ*lacX7, galE, galK, thi, rpsL, strA* 4, Δ*phoA*(pvuII), Δ*ompT*	(42)
E. coli BL21(DE3) Δtig	F $^-$, *ompT, gal, dcm, lon, hsdS*$_B$($r_B{}^-$ $m_B{}^-$) (DE3) Δ*tig*	(24)
pET36	proOmpA(245C)	(43)
pEK504	proOmpA-DHFR(282C)	(26)
pMKL18	SecA	(44)
pHKSB366	SecB	(20)
pEK1	Cysteine-less SecY	(22)
pEK20	Cysteine-less SecYEG	(22)
pEK20-65C	SecY(N65C)EG	(6)
pEK20-67C	SecY(F67C)EG	(6)
pEK20-68C	SecY(F68C)EG	This study
pEK20-69C	SecY(F69C)EG	This study
pEK20-255C	SecY(R255C)EG	This study
pET650	SecY(I278C)EG	(28)
pET84	SecY(G295C)EG	(45)
pEK20-65C-404C	SecYEG(404C-65C)EG	(6)
pUC19Strep$_3$ FtsQSecM	RNC-FtsQ-108	(23)
pEK764	RNC-FtsQ-87	This study

MATERIALS AND METHODS

Chemicals and Biochemicals—ProOmpA, proOmpA-DHFR (18), SecA (19), and SecB (20) were overexpressed and purified as described. Overexpression of SecYEG and isolation of inner membrane vesicles (IMVs) were performed as described (18). For translocation assays, proOmpA-(245C) and proOmpA-DHFR(S282C/C290S/C302S) were labeled with fluorescein-5-maleimide (Invitrogen) (21). *N*-((2-(Iodoacetoxy)ethyl)-*N*-methyl)amino-7-nitrobenz-2-oxa-1,3-diazole (NBD ester) was also from Invitrogen. DNA restriction enzymes were purchased from Fermentas. All other chemicals were from Sigma.

Strains and Plasmids—All *E. coli* strains and plasmids are listed in Table 1. Cloning techniques were performed using DH5α cells. Site-directed mutagenesis according the Stratagene QuikChange® kit was used to introduce cysteines in the template vector pEK1 (22). Subsequently, the NcoI-ClaI Secy fragment containing the unique cysteine was cloned in the expression vector pEK20. For the plasmid encoding FtsQ RNCs of 87 residues preceded by a triple strep tag, the Pst1-EcoRV fragment of pUC19Strep$_3$FtsQSecM (23) was exchanged with fragments coding for FtsQ (3–51) yielding pEK764. All plasmids were verified by sequence analysis.

Fluorescent Labeling, Purification, and Reconstitution of SecYEG—IMVs (1 mg) were resuspended into 1 ml of 50 mM Tris-HCl, pH 8.0. Thiol groups were reduced with 2 mM Tris(2-carboxyethyl)phosphine and labeled with 4 mM NBD ester for 2 h under continuous shaking at 4 °C. Labeling with fluorescein-5-maleimide was performed for 15 min at 20 °C. The reaction was quenched by 12 mM glutathione. IMVs were pelleted by ultracentrifugation at 100,000 rpm in a TLA 100.4 rotor (Beckman) and resuspended in 50 mM Tris-HCl, pH 8.0, and 20% (v/v) glycerol.

To immobilize the plug domain, IMVs containing SecY(404C-65C)EG were either treated 1 mM sodium tetrathionate (NaTT) to induce cross-linking. Controls received 10 mM DTT. Cross-linking efficiency was analyzed by an OmpT assay as described (14).

For SecYEG purification, IMVs containing overexpressed, fluorescently labeled or cross-linked SecYEG were solubilized in 50 mM Tris-HCl, pH 8.0, 10% (v/v) glycerol, 100 mM NaCl, 2% (w/v) β-D-dodecylmaltoside (DDM) for 30 min. Non-soluble material was removed by tabletop centrifugation at maximum speed for 10 min. Solubilized proteins were incubated with 75 μl of nickel-nitrilotriacetic acid-agarose beads (Qiagen) for 1 h at 4 °C. The beads were pelleted and washed 2 times with 50 mM Tris-HCl, pH 8.0, 10% (v/v) glycerol, 100 mM NaCl, and 0.1% (w/v) DDM. SecYEG was eluted with the same buffer supplemented with 50 mM EDTA. The eluate was analyzed by 15% SDS-PAGE, and labeling efficiencies were determined by absorption spectra.

SecYEG was reconstituted by incubating 100 μl of 5 μM purified SecYEG with 100 μl of 4 mg/ml acetone/ether-washed *E. coli* phospholipids (Avanti) in 0.5% (v/v) Triton X-100 for 30 min on ice. Bio-Beads (Bio-Rad) were washed twice with methanol, twice with demineralized water, and twice with buffer A (50 mM Tris-HCl, pH 8.0, 50 mM KCl), and 100 mg was added to the liposome/SecYEG mixture. Samples were incubated at 4 °C overnight. Proteoliposomes were separated from the Bio-Beads and collected by ultracentrifugation at 100,000 rpm in a TLA 100.4 rotor (Beckman). Pellets were resuspended in 100 μl of buffer A and analyzed on 15% SDS-PAGE.

Ribosome and RNC Isolation—E. coli BL21(DE3)Δtig::Kan (24) was transformed with pUC19Strep$_3$FtsQSecM (23) or pEK764 and grown at 30 °C to an $A_{600\,nm}$ of 0.5 in 1 liter LB supplemented with 100 μg/μl of ampicillin. Cells were induced with 0.5 mM isopropyl 1-thio-β-D-galactopyranoside for 30 min and quickly cooled down by use of ice cubes. For the collection of non-translating (control) ribosomes, cells were not induced. After harvesting, cells were lysed according to Evans *et al.* (25). The cell debris was pelleted by centrifugation (twice at 30,000 × *g*, 4 °C, and 30 min) using a MLA80 rotor (Beckman). The clear lysate was collected and laid on a 1 M sucrose cushion prepared in buffer R (50 mM Tris-HCl, pH 7.5, 150 mM KCl, and 10 mM $MgCl_2$). After centrifugation (112,000 × *g*, 4 °C, 17 h), the ribosomal pellet was dissolved in cold buffer R. Non-translating ribosomes were stored in −80 °C. For labeling, the ribosomes were reduced for 15 min at 4 °C with 1 mM Tris(2-carboxyethyl)phosphine and labeled for 1 h at 4 °C with 50 μM fluorescein-5-maleimide. Ribosomes containing RNCs were loaded on a StrepTactin column (IBA). After washing the column with 2 column volumes of buffer R containing 0.5 M KCl and 5 column volumes of buffer R, ribosome nascent chains were eluted with 2 column volumes of buffer R containing 2.5 mM desthiobiotin. The eluate was concentrated by centrifugation (140,000 × *g*, 4 °C, 3 h) and dissolved overnight on ice in buffer R. The ribosome concentration was determined using $A_{260\,nm}$. The presence of RNCs was confirmed by SDS-PAGE followed by Western blotting using an antibody against the strep tag (IBA).

In Vitro Translocation Assays—Translocation assays with SecYEG proteoliposomes were done as described (21, 26). To determine the efficiency of SecYEG trapping by proOmpA-DHFR, translocation reactions with unlabeled proOmpA-DHFR were scaled up twice. Either ATP or ADP was added, and after 10 min the samples were loaded on a 50-μl cushion of 15% (v/v) glycerol and 50 μM methotrexate and centrifuged in a Beckman Airfuge using the A100/30 rotor for 20 min at 25 p.s.i. Pellets were resuspended in 50 μl of translocation buffer supplemented with fluorescein-labeled proOmpA. Samples were briefly sonicated for 1 min in a Branson 1510 water bath, and the translocation of fluorescein-labeled proOmpA was started with ATP and analyzed as described above.

Ribosome Sedimentation Assay—Fluorescein-labeled or unlabeled ribosomes and RNCs were mixed with SecYEG proteoliposomes to concentrations of 50 and 100 nM, respectively, in a total volume of 20 μl in buffer R (50 mM Tris-HCl, pH 7.5, 10 mM $MgCl_2$, and 150 mM KCl). After 30 min of incubation on ice, DDM was added to an end concentration of 0.5% (w/v). After 15 min on ice, reactions were mixed with an equal volume of buffer R containing 17.5% (w/v) sucrose. Samples were loaded on top of a sucrose cushion consisting of 800 μl of buffer R and 17.5% (w/v) sucrose and centrifuged in a TLA 100.2 rotor in a Beckman desktop ultracentrifuge for 1 h at 200,000 × *g*. Supernatant and pellet fractions were collected and analyzed by SDS-PAGE. Gels were analyzed by fluorescent imaging or with silver staining.

Fluorescence Assay—Spectrophotometric analysis of the NBD fluorescence was performed on an Aminco Bowman series II spectrophotometer using excitation and emission wavelengths of 478 and 525 nm, respectively. The slit width was set at 4 nm, and the temperature was kept at 37 °C. Before measurements, proteoliposomes were sonicated for 1 min in a Branson 1510 water bath for dispersion and to reduce the light scattering. All reactions were started after 2 min by the addition of 2 mM nucleotide and continued for 10 min. Fluorescence was corrected for background by subtracting signals for proteoliposomes with cysteine-less SecYEG that was preincubated with NBD as described above. Real time fluorescence measurements translocation reactions were performed in a 150-μl volume using unlabeled proOmpA-DHFR or proOmpA as substrate. Reactions contained 75 pmol of SecA and 15 pmol of SecYEG in proteoliposomes in 20 mM HEPES-KOH, pH 7.0, 50 mM KCl, and 10 mM $MgCl_2$. When indicated, reactions were supplemented with 1 mM ADP, 2 mM $BeSO_4$, and 8 mM NaF. For ribosome and RNC binding, 30 pmol of control ribosomes or RNCs were added to 10 pmol of SecYEG in proteoliposomes in buffer R.

Time-correlated Single Photon Counting—Time correlated single photon counting measurements were performed using a Coherent 9000 laser operating at a frequency of 1.9 MHz with a light intensity of 10 microwatts. The excitation wavelength was set to 467 nm, and for emission a 515-nm cutoff filter was used. Data normally were collected to a peak value of 10^3 counts. The fluorescence decay curve was fitted by least-squares minimization to sums of two exponentials. Average fluorescence lifetime was calculated as described by Lakowicz (27).

RESULTS

Site-specific Introduction of NBD Fluorophores in the SecY Plug Domain—To explore the conformational dynamics inside the SecYEG pore, we introduced unique cysteines in structural regions of SecY to enable the specific introduction of the environment-sensitive fluorophore NBD. Based on the *M. jannaschii* SecYEβ structure (2), four positions were chosen within

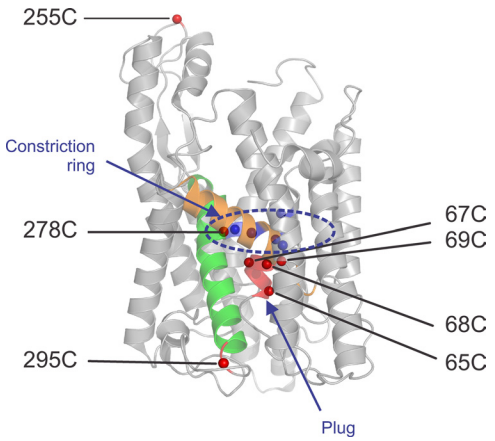

FIGURE 1. **Positions of the cysteine mutations (*red beads*) introduced into the *E. coli* SecY as mapped on the *M. jannaschii* SecY structure.** The plug is shown in *red*, and lateral gate TMS2b and -7 are shown in *orange* and *green*, respectively. Residues that form the hydrophobic constriction ring are represented as *blue beads*.

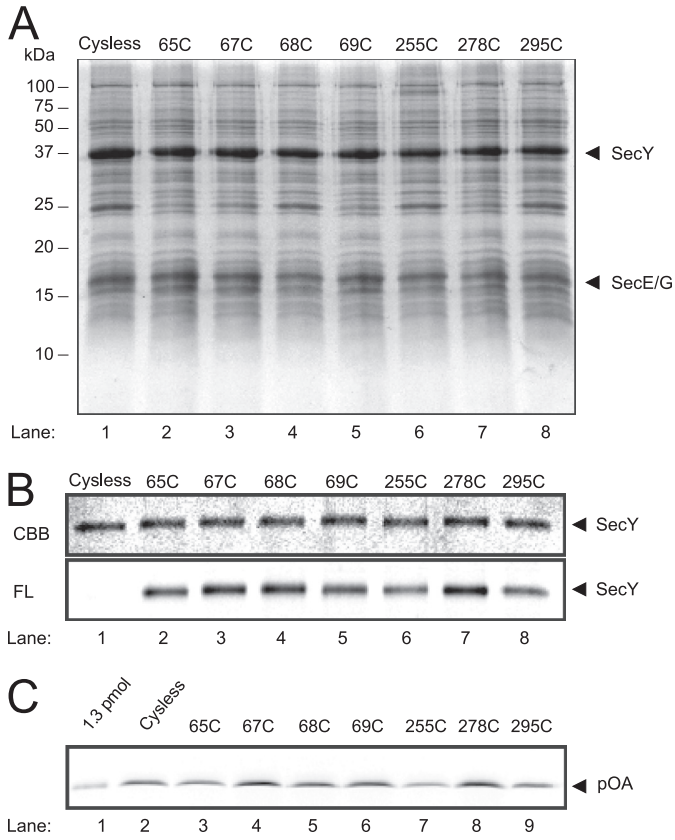

FIGURE 2. *A*, protein levels of the indicated SecYEG complexes are shown. IMVs were isolated from cells overexpressing the various SecYEG complexes, loaded on SDS-PAGE followed by staining with Coomassie Brilliant Blue. *B*, proteoliposomes containing the different NBD-labeled single cysteine SecYEG complexes were analyzed on SDS-PAGE and stained with Coomassie Brilliant Blue (*CBB*) or fluorescent imaging at 510 nm. *C*, translocation of fluorescein-proOmpA (*pOA*) by proteoliposomes reconstituted with NBD-labeled Cys-less and single cysteine SecYEG complexes is shown.

TABLE 2

Efficiency of NBD labeling of purified single cysteine SecYEG complexes

The NBD labeling efficiency was determined by measurements of the absorbance at 280 and 478 nm for SecYEG and NBD, respectively. Extinction coefficients used were 70,820 and 25,000 M^{-1} cm^{-1}, respectively.

SecY mutant	SecYEG	NBD	NBD/SecYEG ratio
	μM	μM	
Cys-less	3.9	0.3	0.06
65C	4.2	4.0	0.97
67C	4.0	4.0	1.00
68C	4.3	4.1	0.97
69C	3.9	4.3	1.09
255C	4.2	3.9	0.93
278C	4.3	4.1	0.94
295C	4.1	3.7	0.90

the plug and one in the pore constriction ring (Fig. 1). Control cysteines were introduced in the cytoplasmic and periplasmic loop between TMS6/7 and TMS5/6, respectively. Each of the mutant SecYEG complexes was well expressed to levels comparable with that of the cysteine-less SecYEG complex (Fig. 2*A*). The IMVs were labeled with NBD and solubilized with the detergent dodecylmaltoside whereupon the His-tagged SecYEG complex was purified by nickel-nitrilotriacetic acid affinity chromatography. Purified complexes were analyzed spectrometrically to examine the extent of NBD labeling. For each of the cysteine mutants of SecY, a near to stoichiometric labeling with NBD was achieved (Table 2). In contrast, negligible labeling of the cysteine-less SecY control was observed. Analysis of proteoliposomes reconstituted with NBD-labeled SecYEG complexes by SDS-PAGE revealed different fluorescence levels (Fig. 2*B*) despite equal protein loading. This indicates that the NBD positions monitor different environments. To examine if the introduction of a unique cysteine and its labeling with NBD has any influence on functionality of the SecYEG complex, proteoliposomes were tested for the translocation of fluorescein-labeled proOmpA. All labeled mutants were active for translocation (Fig. 2*C*), with the SecY(67C)EG and SecY(278C) complexes showing a slightly elevated activity. These SecY mutants were reported to display a prl phenotype (28, 29), which is associated with an elevated protein translocation activity. A similar pattern of activity was observed when the mutants were not labeled with the fluorophore (data not shown). Taken together these data demonstrate that the selected cysteine mutants of SecY remain active after fluorescent labeling with NBD.

The Plug Domain Is in an Apolar Environment—To obtain insight in the polarity of the environment of the NBD fluorophore at different locations within the SecYEG complex, we employed time correlated single photon counting to measure the fluorescence lifetimes (27). Typical fluorescence decay curves are shown in Fig. 3*A* for NBD at position 278 and 255, predicted to be in a hydrophobic and hydrophilic environment, respectively. Decay curves were fitted to double exponentials, and average fluorescence lifetimes (τ_{avg}) were calculated as a measure of polarity. As expected, τ_{avg} of NBD at positions 255 and 295 of SecY is short, *i.e.* 4–5 ns, as these residues are solvent-exposed at the cytosolic and periplasmic membrane face, respectively (Fig. 3*B*). On the other hand, when the NBD is in the hydrophobic constriction ring, a long τ_{avg} of about 7 ns is recorded. Also the positions in the plug domain (residues 67, 68, and 69) indicate a long τ_{avg} consistent with exposure to a hydrophobic environment. Position 65 that is further away from the constriction ring (Fig. 1) yielded a lower τ_{avg} value and thus is more exposed to solvent. Taken together, the τ_{avg} observed for the NBD fluorescence at different locations of

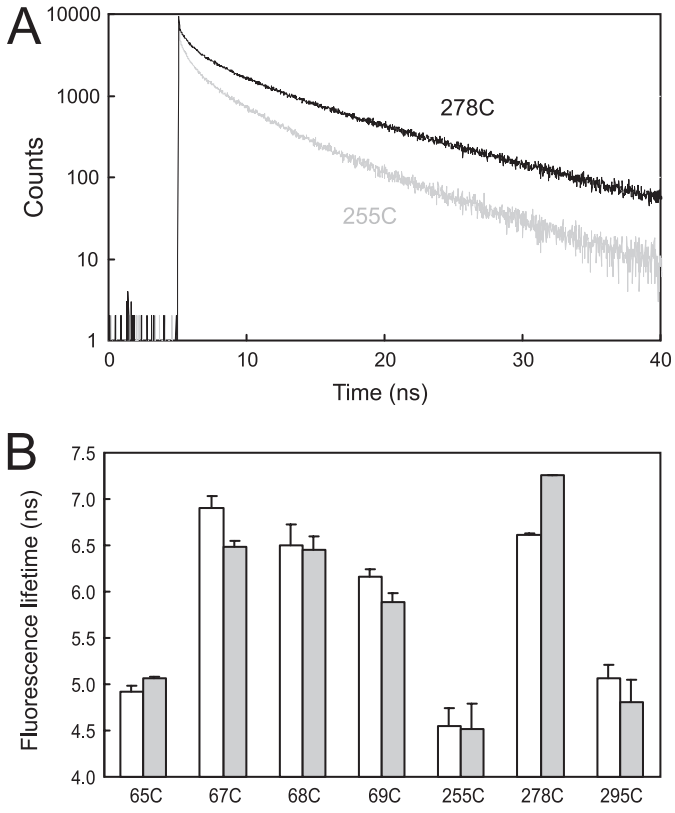

FIGURE 3. **Formation of a proOmpA-DHFR translocation intermediate in SecYEG proteoliposomes.** *A*, shown is translocation of fluorescein-proOmpA-DHFR in the proteoliposomes containing different NBD-labeled SecYEG complex and the formation of a translocation intermediate (I_{37}). Reactions were started with either ADP (no translocation) or ATP (translocation intermediate). *B*, formation of a proOmpA-DHFR translocation intermediate in SecYEG proteoliposomes results in an efficient block in translocation sites. SecYEG proteoliposomes were first incubated with proOmpA-DHFR in the presence of SecA and either ADP or ATP as energy source. Next, SecYEG proteoliposomes were collected by sedimentation through a glycerol cushion, resuspended, and subjected to another round of translocation of fluorescein-proOmpA in the presence of SecA and ATP.

SecY are in agreement with the structure of the closed state of the SecYEG complex.

Conformational Dynamics of the SecY Plug during Protein Translocation—To analyze the conformational dynamics of the plug, NBD fluorescence intensities were recorded under various conditions. First, an "open" state of SecYEG was induced by the partial translocation of proOmpA fused at its C terminus to folded dihydrofolate reductase (DHFR) (30, 31) into the proteoliposomes reconstituted with NBD-labeled SecYEG as described previously (26) (Fig. 4*A*). The preprotein intermediates effectively blocked the translocation of proOmpA in a second round of translocation (Fig. 4*B*). By real time monitoring of the NBD fluorescence of the plug domain positions, formation of the proOmpA-DHFR translocation intermediate was followed kinetically. SecYEG proteoliposomes were supplemented with SecA and the SecB:proOmpA-DHFR complex, and translocation was initiated by the addition of ATP. Fig. 5*A* shows a typical fluorescence trace for the NBD-labeled SecY(67C)EG. The fluorescence intensity decreased by 16% upon the formation of the translocation intermediate, suggesting an increased solvent exposure of the NBD group consistent with the fluorescence lifetime experiments. To ensure that the fluorescent change is due to formation of the translocation intermediate and channel opening, control experiments were performed by replacing the ATP for the nucleotides ADP and AMP-PNP or by leaving out proOmpA-DHFR or SecA. Under those conditions, no change in NBD fluorescence was observed (Fig. 5*B*). When instead of proOmpA-DHFR, proOmpA was added, a similar but lesser decrease in NBD fluorescence was noted. Unlike with the trapped translocation intermediate, continuous translocation of proOmpA presumably results in an only partial occupancy of the ensemble of SecYEG channels in time. The above experiments were repeated for all the different NBD-labeled SecYEG proteoliposomes (Fig. 5*C*). A decrease in NBD fluorescence upon the formation of the proOmpA-DHFR translocation intermediate was observed with positions 67 and 69 at the top of the plug domain, whereas an increased fluorescence was noted for position 65, which is located more peripherally. The increased fluorescence at this position suggests a shielding from solvent, *i.e.* relocation to a more hydrophobic environment. These results indicate that the plug domain moves to a different location, away from the hydrophobic constriction ring resulting in a different solvent exposure of the various positions in this domain. On the other hand, the fluorescence intensity of NBD at residue 278 in the hydrophobic constriction ring increases upon the formation of the proOmpA-DHFR translocation intermediate, which was also noted in the fluorescence lifetime measurements. Apparently, the presence of the translocation intermediate in the constriction ring that may function as a hydrophobic gasket causes this increased hydrophobicity. Importantly, τ_{avg} measurements suggest similar changes in solvent exposure (Fig. 3*B*). These data indicate a conformational change in the plug domain upon the formation of a translocation intermediate rendering this region more solvent-exposed.

In the absence of nucleotide or ADP, SecA binding to the SecYEG proteoliposomes results in no appreciable change in NBD fluorescence (Fig. 5*C*). A recent structure of SecYEG with bound SecA in the presence of ADP and beryllium fluoride (13) depicts the channel in a so-called pre-open state with a partial opened lateral gate and a plug that has been released from its central channel position. Indeed, in the presence of ADP-beryllium fluoride, SecA induced an increased NBD fluorescence at plug domain residues 65 and 68, whereas positions 67 and 69 appear invariant (Fig. 5*C*). Binding also caused a small increase in NBD fluorescence at position 278 of the constriction ring and residue 295 in the periplasmic loop. The overall pattern of fluorescent changes is different when compared with the conformational changes induced by proOmpA translocation but support the structural data, indicating a re-allocation of the plug, thus providing structural validation for our fluorescent measurements.

Conformational Dynamics of the SecY Plug upon Ribosome Nascent Protein Binding—During membrane protein insertion, inserting nascent membrane proteins may slide into the membrane via the lateral gate, but it is unclear to what extent the plug domain needs to be re-allocated. To investigate the plug domain movement under those conditions, ribosomes were isolated loaded with a nascent polypeptide of the monotopic integral membrane protein FtsQ with either a length of 87 or

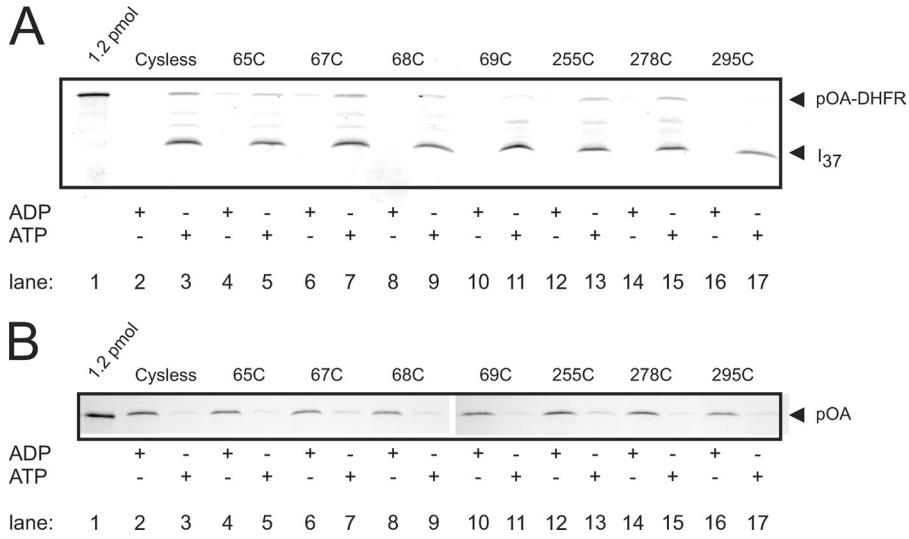

FIGURE 4. **Time-resolved fluorescence spectroscopy of proteoliposomes reconstituted with NBD-labeled single cysteine SecYEG complexes.** *A*, NBD fluorescence decay curves were obtained from time-correlated singe photon counting experiments using proteoliposomes containing the SecY(I278C)EG or SecY(R255C)EG complex. *B*, averaged NBD fluorescence lifetimes of the indicated SecYEG complexes reconstituted in proteoliposomes that were incubated with SecA and proOmpA-DHFR (*pOA*) in the presence of ADP (no translocation, *white bars*) or ATP (translocation intermediate, *gray bars*).

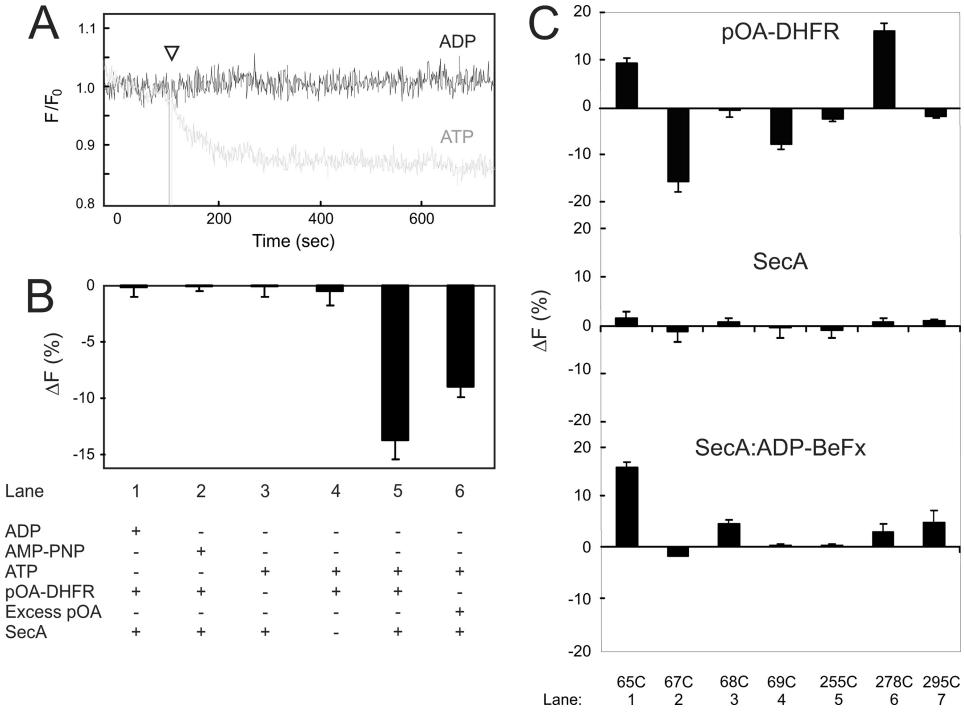

FIGURE 5. **Conformational dynamics of the SecYEG complex labeled at specific cysteine positions with NBD upon protein translocation.** *A*, shown is real-time spectrophotometric detection of the fluorescence of the NBD-labeled SecY(67C)EG complex reconstituted into proteoliposomes. Samples were incubated with SecA and proOmpA-DHFR, and translocation was induced by the addition of ATP (*gray*, translocation intermediate) or ADP (*black*, no translocation). *B*, shown are fluorescence changes of the NBD-labeled SecY(67C)EG complex reconstituted into proteoliposomes in the presence of different nucleotides, SecA, and/or the preprotein proOmpA-DHFR (*pOA-DHFR*) or proOmpA (*pOA*). *C*, fluorescence changes of NBD-labeled single cysteine SecYEG complexes reconstituted into proteoliposomes upon the binding of SecA in the absence or presence of ADP and beryllium fluoride (*BeFx*) and upon the formation of a proOmpA-DHFR translocation intermediate.

108 residues. The nascent chains contain a SecM stalling sequence, a TMS that functions as an N-terminal signal anchoring domain, and an N-terminal strep tag (23, 32). FtsQ87 exposes only the TMS from the ribosomal exit tunnel, whereas FtsQ108 exposes an additional stretch of polar amino acids, but both TMS are inserted into the membrane in the SecYEG-bound state. As a control we isolated ribosomes from cells that did not express the stalled FtsQ truncate. Ribosomes and RNCs were analyzed on SDS-PAGE and immunoblotted using a strep tag antibody (Fig. 6*A*). Ribosomes were also labeled fluorescently with fluorescein-maleimide and visualized in gel using fluorescent imaging. The binding of SecYEG to ribosomes and RNCs was analyzed by a co-sedimentation assay. In this assay, the SecYEG proteoliposomes and ribosomes or RNCs were mixed, subsequently solubilized with DDM, and sedimented through a sucrose cushion. The pellet fraction containing the ribosomes was subsequently analyzed for the co-sedimented SecYEG complex. With empty ribosomes, hardly any SecYEG

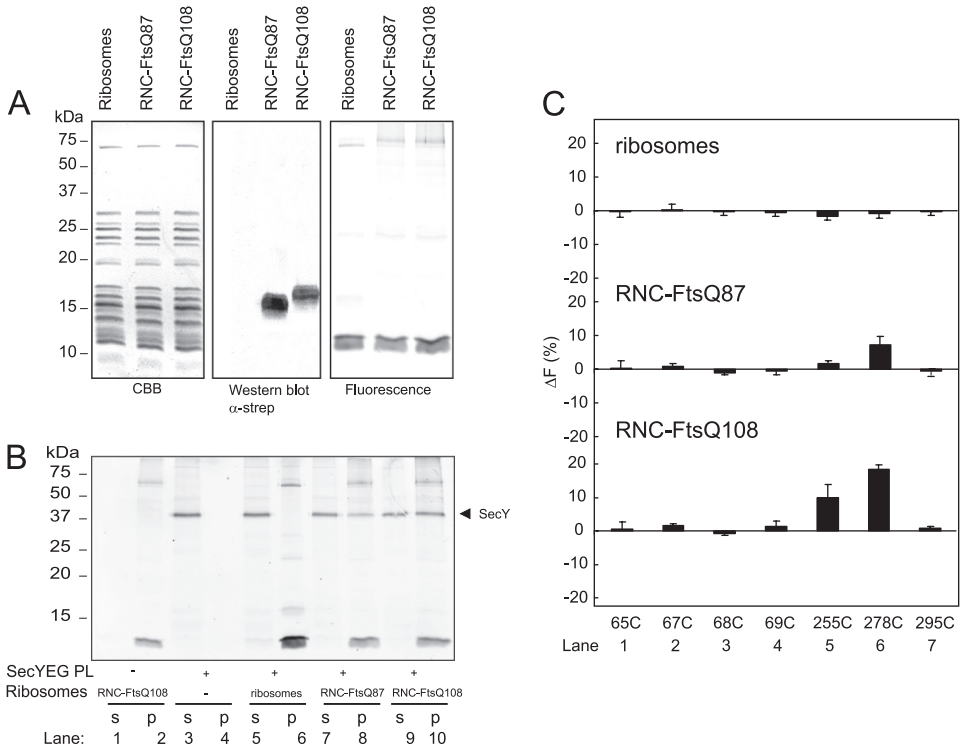

FIGURE 6. **Conformational dynamics of the SecYEG complex labeled at specific cysteine positions with NBD upon ribosome-mediated membrane protein insertion.** *A*, shown is SDS-PAGE analysis and Coomassie Brilliant Blue (*CBB*) staining, Western blotting and strep-tag detection, and fluorescent imaging of isolated ribosomes and RNCs labeled with fluorescein. RNC-FtsQ87 and FtsQ108 represent SecM-stalled ribosome bound nascent chains of FtsQ with a length of 87 or 108 amino acids long, respectively. *B*, binding of ribosomes and RNCs to SecYEG proteoliposomes was analyzed by co-sedimentation. Fluorescein-labeled ribosomes, RNC-FtsQ87, or RNC-FtsQ108 were incubated with fluorescein-labeled SecY(67C)EG proteoliposomes, solubilized with 0.5% DDM, and layered on top of a sucrose cushion. Samples were subjected to ultracentrifugation, and supernatant (*S*) and pellet (*P*) fractions were analyzed on SDS-PAGE and fluorescent imaging. *C*, shown are fluorescence changes of NBD-labeled single cysteine SecYEG complexes reconstituted into proteoliposomes upon the binding of ribosomes, RNC-FtsQ87, or RNC-FtsQ108.

complex was found in the pellet (Fig. 6*B*, *lane 6*). However, in the presence of a FtsQ nascent chain, efficient co-sedimentation of SecYEG and ribosomes was observed (Fig. 6*B*, *lane 8* and *10*). To examine the plug domain conformation upon ribosome binding, proteoliposomes containing the different NBD-labeled SecYEG complexes were incubated with control ribosomes and RNCs. The addition of the control ribosomes did not result in any change in NBD fluorescence (Fig. 6*C*), consistent with the notion that these ribosomes do not bind SecYEG. The addition of the FtsQ87 and FtsQ108 RNCs resulted in a significant increase in the NBD fluorescence at residue 278 at the constriction ring indicative of an increased hydrophobicity of its environment. This fluorescence increase was higher with FtsQ108 RNCs as compared with the FtsQ87 RNCs. In a recent cryo-EM study on FtsQ108 RNCs bound to SecYEG reconstituted in nanodiscs, it was found that the hydrophobic TMS of FtsQ intercalates between TMS2 and TMS7 of SecYEG, the proposed lateral gate (17). The chain appears to be in direct contact with the constriction ring including residue 278, suggesting that the polypeptide interaction causes the observed increase in hydrophobicity. In contrast, with FtsQ87 RNCs, insertion may not yet be completed, and a lower level of interaction is observed. Importantly, no significant changes are observed in the NBD fluorescence of the plug domain upon the interaction of SecYEG with FtsQ87 and FtsQ108 RNCs. This suggests a major difference in plug domain dynamics when RNCs bind the SecYEG complex as compared with SecA-mediated protein translocation.

Because our data suggest little mobility of the plug domain upon the membrane insertion of the FtsQ nascent chain, insertion was examined in the SecY(404C-65C)EG mutant in which the tip of the plug domain can be immobilized to TMS10 by disulfide bond formation as shown previously (6). Herein, the mutant was oxidized with the hydrophilic agent NaTT. Intramolecular disulfide bond formation was assayed with the OmpT protease that cleaves SecY between arginine 255 and 256 in the cytoplasmic loop that connects TMS6 and TMS7. In the absence of a cross-link, this results in the formation of an N- and C-terminal SecY fragment with calculated molecular masses of 28 and 20 kDa, respectively. On SDS-PAGE, these fragments migrate at apparent molecular masses of 25 and 18 kDa, respectively (Fig. 7*A*, *lane 2*). Upon oxidation of the cysteines in TMS2a (plug) and TMS10, OmpT treatment no longer resulted in a cleaved product, showing the full-length SecY (Fig. 7*A*, *lane 4*), indicative of an efficient immobilization of the plug domain to TMS10. To examine insertion of the FtsQ nascent chain, the binding or RNCs to the cross-linked SecY(404C-65C)EG mutant complex was analyzed by the sedimentation assay described in the previous section. Both the cross-linked and non-cross-linked SecYEG mutant showed a similar pattern in ribosome and RNC co-sedimentation (Fig. 7*B*). Whereas little co-sedimentation was observed with control ribosomes, an

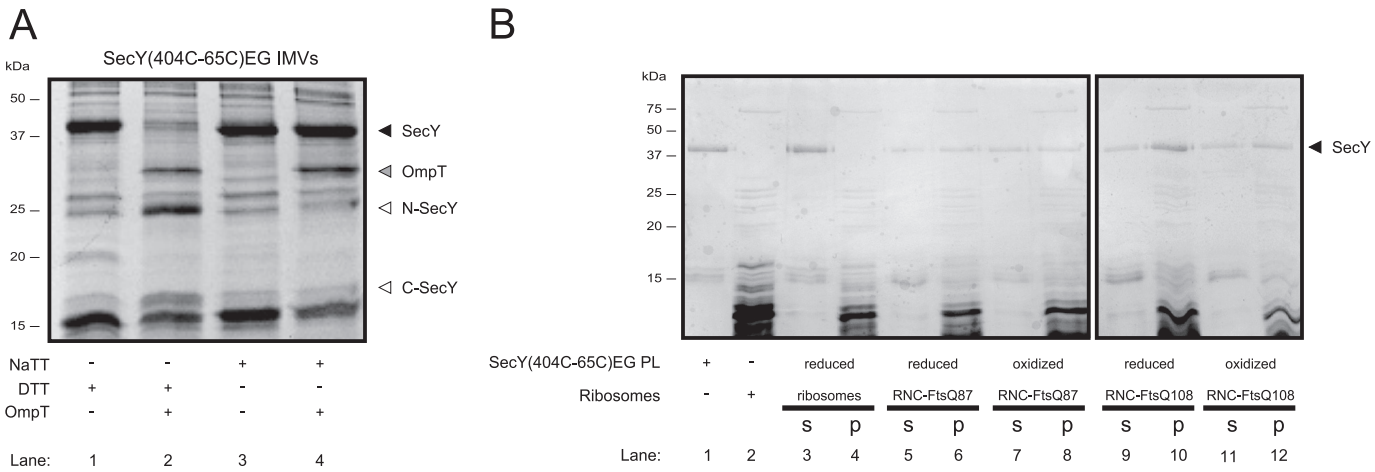

FIGURE 7. **Binding and insertion of FtsQ RNCs to SecY(404C-65C)EG mutant with an immobilized plug domain.** *A*, IMVs harboring overexpressed levels of SecYEG(404C-65C)EG were treated with 10 mM DTT (non-cross-linked) or 1 mM NaTT (cross-linked), and the cross-linking efficiency was checked by OmpT treatment. *B*, binding of ribosomes and RNCs to SecY(404C-65C)EG proteoliposomes that were treated with 10 mM DTT (non-cross-linked) or 1 mM NaTT (non-cross-linked) was analyzed by co-sedimentation as described in the legend to Fig. 6. Supernatant (*S*) and pellet (*P*) fractions were analyzed by SDS-PAGE followed by silver staining.

efficient interaction occurred with the FtsQ RNCs irrespective the immobilization of the plug domain. The data suggest that immobilization of the plug domain does not block the insertion of the FtsQ nascent chain.

DISCUSSION

In this study we analyzed the conformational changes within the plug domain region of the SecYEG protein-conducting channel at different stages of protein translocation and insertion. Herein, unique cysteines were introduced in the plug domain as well as in the hydrophobic constriction ring and at SecY loops exposed to the cytoplasmic or periplasmic side of the membrane. These cysteines were labeled with the environment-sensitive NBD fluorophore. Fluorescence lifetime analysis confirmed that the polarity sensed by the NBD probes agrees with the predicted polarity of the regions as derived from the *M. jannaschii* SecYEβ structure (2). The average fluorescence lifetimes ranged from ~4 ns for the solvent-exposed regions at the periplasmic or cytoplasmic side of the channel up to ~7 ns for residues in the hydrophobic constriction ring and the top of the plug domain facing the constriction ring. The fluorescence lifetime of NBD depends not only on the polarity of the environment but also on the hydrogen-bonding donor capacity of the solvent. Previous studies have shown that when a NBD fluorophore is exposed to different protic and aprotic solvents, the fluorescence lifetime ranges from ~1 ns for purely water to >10 ns in ethyl acetate (33, 34). A fluorescent lifetime of around 7 ns is observed when NBD is dissolved in butanol, a value that corresponds to the fluorescence lifetimes observed for positions within or close to the hydrophobic constriction ring, which consists mainly of isoleucines. The fluorescence lifetime of 4 ns of the surface-exposed NBD positions suggests that these residues are partly shielded to water by other amino acids possibly because of a high flexibility of the loop regions.

The formation of a stable proOmpA-DHFR translocation intermediate resulted in specific changes in the NBD steady state fluorescence and lifetime and indicate conformational changes in the pore region (Fig. 3*B*). Although the fluorescence lifetime changes are relatively small, it is important to stress that with the SecYEG proteoliposomes, about 50% of the SecYEG complexes are wrongly oriented and cannot bind SecA. They thus do not take part in the translocation reaction, whereas the recorded life time is the average of the entire SecYEG population. The NBD at the plug domain residues 67 and 69 showed a small decrease in fluorescence lifetime, indicating a greater solvent exposure. On the other hand, residue 68 remains in the same hydrophobic environment. These findings support our previous finding that the plug domain remains largely inside the channel during translocation (6) rather than being completely transferred to the back of the C-terminal tail of SecE, which would be signified by a much greater solvent exposure. Residue 278 is located on TMS7 that forms the lateral gate together with TMS2. The increase of fluorescence lifetime at this location can be explained with the intercalation of the hydrophobic signal sequence of proOmpA-DHFR (35). Essentially, similar results were obtained when instead of fluorescence lifetime, the NBD fluorescence was monitored. With the plug position 67, a maximal reduction by 16% of the NBD fluorescence level was observed upon the formation of the proOmpA-DHFR translocation intermediate. When corrected for the fraction of correctly oriented SecYEG complexes reconstituted into the proteoliposomes, the decrease is around 32%. Previous work on proteins labeled with NBD showed an almost total reduction in fluorescence when the fluorophore was transferred from a polar to an aqueous environment (26, 36). Therefore, the observed changes in fluorescence indicate that the plug domain remains in a relatively hydrophobic environment and is not entirely solvent-exposed. Molecular dynamics simulations that examined the influence of mutations in the SecY channel on the position of the plug showed that hydration of the plug domain already occurs even after a small relocation within the channel (37). This hydration is likely responsible for the decrease in NBD fluorescence observed in this study. Remarkably, when stable SecA binding in the presence of ADP and beryllium fluoride was induced, a different

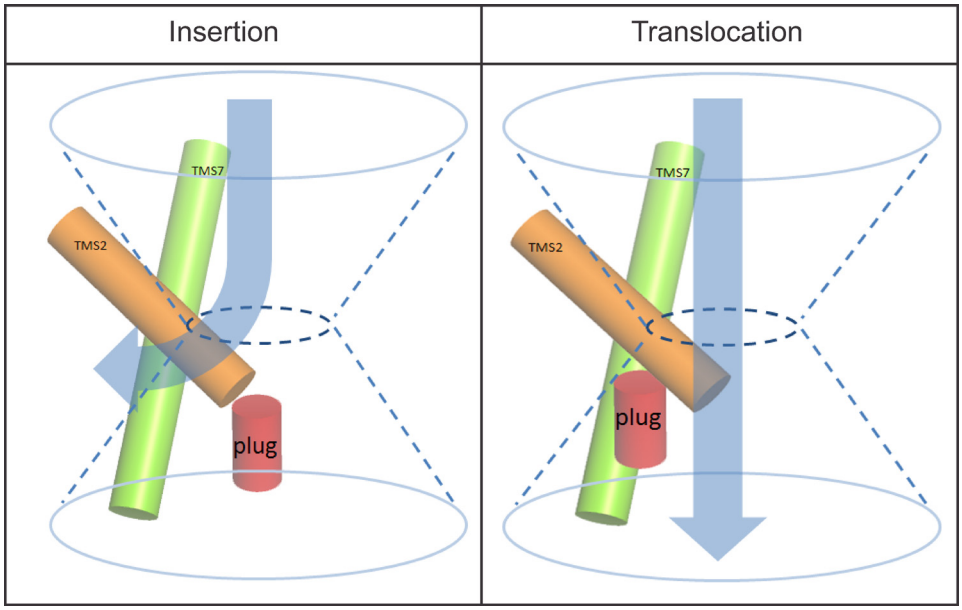

FIGURE 8. **Model for the plug domain movement during membrane protein insertion and protein translocation.**

pattern in the NBD fluorescence of the plug domain was noted. Little change in NBD fluorescence occurred with position 67 at the top of the plug domain, but rather, an increased NBD fluorescence was monitored at residues 65 and 68, suggesting a decreased solvent exposure of these residues. Because the hydrophobicity for residue 65 is low, as signified by its fluorescence lifetime, the SecA-induced increased fluorescence suggests a shielding from water molecules or relocation toward more hydrophobic residues. In conjunction with the small fluorescence increase of NBD at residue 295, it appears that the periplasmic side of the translocation funnel is constricted, resulting in a lower penetration of solvent.

Structural data indicate that SecA binding in the presence of ADP-beryllium fluoride induces the relocation of the plug domain from its central position to a region near to the periplasmic end of the lateral gate (13). In this so-called pre-open state, and a greater solvent exposure of the plug domain is expected. However, the structural data were obtained in the absence of the lateral pressure of the membrane, and this may have distinct effects on SecYEG conformation. Therefore, we conclude that the plug domain of the SecYEG channel is highly dynamic and undergoes progressive conformational changes during SecA-mediated protein translocation when the channel switches from its closed to the pre-open and open state.

To examine the conformational dynamics of the plug domain during membrane protein insertion, the SecYEG complex was incubated with ribosomes and ribosome nascent chains of the monotopic membrane protein FtsQ that expose the N-terminal signal-anchoring domain. Such complexes have previously been investigated by cryo-EM and cross-linking analysis. Little interaction between SecYEG and non-translating ribosomes was observed, but the presence of a nascent chain strongly stimulated the interaction (Fig. 6*B*). This contrasts previous studies that report binding of non-translating ribosomes to the purified SecYEG complex (38, 39). The apparent discrepancy likely results from the lower ribosome concentrations used in our sedimentation experiments and the use of SecYEG reconstituted into a lipid bilayer. This in contrast to the EM studies that use a large excess of ribosomes and SecYEG complex in detergent solution. Therefore, we conclude that non-translating ribosomes are poor binding ligands to the SecYEG complex. Our data further suggest that FtsQ108 RNCs represent a better binding ligand for SecYEG than the shorter chain FtsQ87 RNC. Likely, membrane and/or channel insertion has progressed further with the longer FtsQ nascent chain. In agreement with our binding studies, no change in NBD fluorescence was observed when the SecYEG complexes were incubated with non-translating ribosomes. On the other hand, both the FtsQ108 and FtsQ87 RNCs induced an increased NBD fluorescence at residues 255 and 278. Residue 255 is located in the loop between TMS6 and -7 and likely directly interacts with the region surrounding the ribosomal exit tunnel (17). This may cause a shielding of this position for water molecules; hence, an increased NBD fluorescence. The increase at residue 278 might be induced by the hydrophobic anchoring domain, which is believed to intercalate between TMS2 and TMS7. Closer examination of the EM densities points out the hydrophobic segment from the nascent chain is in close proximity with residue 278, thereby adding to the already hydrophobic environment of the constriction ring. Remarkably, there is no significant change in fluorescence of any of the NBD positions located on the plug domain upon binding of the RNCs. Because it is very unlikely that all four positions of the plug domain would have moved to an environment with the exact same polarity as the original position, we therefore conclude that during the insertional stage of a nascent membrane protein, the plug domain does not move from its central position. In the cryo-EM structure of the mammalian Sec61 complex associated with a RNC (40), which reflects a later stage in the translocation process, the channel was found to be in a conformation where the lateral gate was closed. In this structure the plug domain was not clearly resolved, although some densities were unaccounted for.

The difference in behavior of the plug domain reported in this study suggests distinct roles of this region in membrane protein insertion and protein translocation. The latter is a vectorial process and requires that the plug domain vacates the central pore position and thus needs to move to a more peripheral location as also suggested by various cross-linking studies. However, with membrane protein insertion, the hydrophobic TMS needs to slide into the membrane according to a lateral insertion mechanism. Because the TMS of FtsQ needs to be inserted rather than translocated, the plug domain may remain at its position near the hydrophobic constriction ring and thus contributes to a vectorial seal of the pore. A recent molecular simulation study suggests that the plug may even play a role in guiding TMSs in the lipid bilayer (12). When a hydrophobic polypeptide segment was inserted in this simulation, the plug domain stayed at a location below the constriction ring and seemed to guide the membrane segments into the lipid bilayer. On the other hand, a more polar polypeptide segment caused the displacement of the plug from its central pore position. It was suggested that the plug acts like a kind of rudder that directs hydrophobic and hydrophilic into and across the lipid bilayer, respectively (Fig. 8). Our studies provide evidence for a functional difference in plug domain dynamics depending on the mode of translocation and insertion and suggest an active role of the SecYEG pore in directing proteins across and into the membrane.

Acknowledgments—We thank Janny de Wit for construct pET84, Nenad Ban for the vector pUC19Strep$_3$FtsQSecM, and Ben Hesp for assistance with the time correlated single photon counting measurements. We thank Alexej Kedrov for careful reading of the manuscript.

REFERENCES

1. Driessen, A. J., and Nouwen, N. (2008) *Annu. Rev. Biochem.* **77,** 643–667
2. Van den Berg, B., Clemons, W. M., Jr., Collinson, I., Modis, Y., Hartmann, E., Harrison, S. C., and Rapoport, T. A. (2004) *Nature* **427,** 36–44
3. Gumbart, J., and Schulten, K. (2008) *J. Gen. Physiol.* **132,** 709–719
4. Harris, C. R., and Silhavy, T. J. (1999) *J. Bacteriol.* **181,** 3438–3444
5. Tam, P. C., Maillard, A. P., Chan, K. K., and Duong, F. (2005) *EMBO J.* **24,** 3380–3388
6. Lycklama, A., Nijeholt, J. A., Bulacu, M., Marrink, S. J., and Driessen, A. J. (2010) *J. Biol. Chem.* **285,** 23747–23754
7. Junne, T., Schwede, T., Goder, V., and Spiess, M. (2006) *Mol. Biol. Cell* **17,** 4063–4068
8. Maillard, A. P., Lalani, S., Silva, F., Belin, D., and Duong, F. (2007) *J. Biol. Chem.* **282,** 1281–1287
9. Li, W., Schulman, S., Boyd, D., Erlandson, K., Beckwith, J., and Rapoport, T. A. (2007) *Mol. Cell* **26,** 511–521
10. Smith, M. A., Clemons, W. M., Jr., DeMars, C. J., and Flower, A. M. (2005) *J. Bacteriol.* **187,** 6454–6465
11. Duong, F., and Wickner, W. (1999) *EMBO J.* **18,** 3263–3270
12. Zhang, B., and Miller, T. F., 3rd (2010) *Proc. Natl. Acad. Sci. U.S.A.* **107,** 5399–5404
13. Zimmer, J., Nam, Y., and Rapoport, T. A. (2008) *Nature* **455,** 936–943
14. du Plessis, D. J., Berrelkamp, G., Nouwen, N., and Driessen, A. J. (2009) *J. Biol. Chem.* **284,** 15805–15814
15. Egea, P. F., and Stroud, R. M. (2010) *Proc. Natl. Acad. Sci. U.S.A.* **107,** 17182–17187
16. Tsukazaki, T., Mori, H., Fukai, S., Ishitani, R., Mori, T., Dohmae, N., Perederina, A., Sugita, Y., Vassylyev, D. G., Ito, K., and Nureki, O. (2008) *Nature* **455,** 988–991
17. Frauenfeld, J., Gumbart, J., Sluis, E. O., Funes, S., Gartmann, M., Beatrix, B., Mielke, T., Berninghausen, O., Becker, T., Schulten, K., and Beckmann, R. (2011) *Nat. Struct. Mol. Biol.* **18,** 614–621
18. van der Does, C., de Keyzer, J., van der Laan, M., and Driessen, A. J. (2003) *Methods Enzymol.* **372,** 86–98
19. Cabelli, R. J., Chen, L., Tai, P. C., and Oliver, D. B. (1988) *Cell* **55,** 683–692
20. Fekkes, P., de Wit, J. G., van der Wolk, J. P., Kimsey, H. H., Kumamoto, C. A., and Driessen, A. J. (1998) *Mol. Microbiol.* **29,** 1179–1190
21. De Keyzer, J., Van Der Does, C., and Driessen, A. J. (2002) *J. Biol. Chem.* **277,** 46059–46065
22. van der Sluis, E. O., Nouwen, N., and Driessen, A. J. (2002) *FEBS Lett.* **527,** 159–165
23. Schaffitzel, C., and Ban, N. (2007) *J. Struct. Biol.* **158,** 463–471
24. Rutkowska, A., Mayer, M. P., Hoffmann, A., Merz, F., Zachmann-Brand, B., Schaffitzel, C., Ban, N., Deuerling, E., and Bukau, B. (2008) *J. Biol. Chem.* **283,** 4124–4132
25. Evans, M. S., Ugrinov, K. G., Frese, M. A., and Clark, P. L. (2005) *Nat. Methods* **2,** 757–762
26. Bol, R., de Wit, J. G., and Driessen, A. J. (2007) *J. Biol. Chem.* **282,** 29785–29793
27. Lakowicz, J. R. (1999) *Principles of Fluorescence Spectroscopy*, pp. 129–132, Kluwer Academic/Plenum Press, New York
28. Manting, E. H., Kaufmann, A., van der, Does, C., and Driessen, A. J. (1999) *J. Biol. Chem.* **274,** 23868–23874
29. Osborne, R. S., and Silhavy, T. J. (1993) *EMBO J.* **12,** 3391–3398
30. Arkowitz, R. A., Joly, J. C., and Wickner, W. (1993) *EMBO J.* **12,** 243–253
31. Joly, J. C., and Wickner, W. (1993) *EMBO J.* **12,** 255–263
32. Nakatogawa, H., and Ito, K. (2002) *Cell* **108,** 629–636
33. Greenough, K. P., and Blanchard, G. J. (2006) *J. Phys. Chem. B* **110,** 6351–6358
34. Lin, S., and Struve, W. S. (1991) *Photochem. Photobiol.* **54,** 361–365
35. Plath, K., Mothes, W., Wilkinson, B. M., Stirling, C. J., and Rapoport, T. A. (1998) *Cell* **94,** 795–807
36. Ramachandran, R., Tweten, R. K., and Johnson, A. E. (2004) *Nat. Struct. Mol. Biol.* **11,** 697–705
37. Bondar, A. N., del Val, C., Freites, J. A., Tobias, D. J., and White, S. H. (2010) *Structure* **18,** 847–857
38. Ménétret, J. F., Schaletzky, J., Clemons, W. M., Jr., Osborne, A. R., Skånland, S. S., Denison, C., Gygi, S. P., Kirkpatrick, D. S., Park, E., Ludtke, S. J., Rapoport, T. A., and Akey, C. W. (2007) *Mol. Cell* **28,** 1083–1092
39. Prinz, A., Behrens, C., Rapoport, T. A., Hartmann, E., and Kalies, K. U. (2000) *EMBO J.* **19,** 1900–1906
40. Becker, T., Bhushan, S., Jarasch, A., Armache, J. P., Funes, S., Jossinet, F., Gumbart, J., Mielke, T., Berninghausen, O., Schulten, K., Westhof, E., Gilmore, R., Mandon, E. C., and Beckmann, R. (2009) *Science* **326,** 1369–1373
41. Hanahan, D. (1983) *J. Mol. Biol.* **166,** 557–580
42. Baneyx, F., and Georgiou, G. (1990) *J. Bacteriol.* **172,** 491–494
43. Bonardi, F., London, G., Nouwen, N., Feringa, B. L., and Driessen, A. J. (2010) *Angew. Chem. Int. Ed. Engl.* **49,** 7234–7238
44. Klose, M., Schimz, K. L., van der Wolk, J., Driessen, A. J., and Freudl, R. (1993) *J. Biol. Chem.* **268,** 4504–4510
45. Kusters, I., van den Bogaart, G., Kedrov, A., Krasnikov, V., Fulyani, F., Poolman, B., and Driessen, A. J. (2011) *Structure* **19,** 430–439